Supporting Information for

Bio-templated Hybrid Microrobots for Enhanced Photocatalytic Water Remediation under Continuous Magnetic Propulsion

By Fajer Mushtaq,* Xiangzhong Chen,* Silvan Staufert, Harun Torlakcik, Xiaopu Wang, Marcus Hoop, Ann Gerber, Xinghao Li, Jun Cai, Bradley J. Nelson, and Salvador Pané

F. Mushtaq, Dr. X. Chen, H. Torlakcik, X. Wang, Dr. M. Hoop, A. Gerber, Prof. B. J. Nelson, Dr. S. Pané.
Institute of Robotics and Intelligent Systems (IRIS), ETH Zurich, CH-8092 Zurich, Switzerland
E-mail: fmushtaq@ethz.ch, chenxian@ethz.ch

Dr. S. Staufert,
Micro and Nanosystems, ETH Zurich, CH-8092 Zurich, Switzerland.

Dr. X. Li, Prof. J. Cai,
School of Mechanical Engineering and Automation, Beihang University, No. 37 Xueyuan Road, Haidian District, Beijing 100191, China

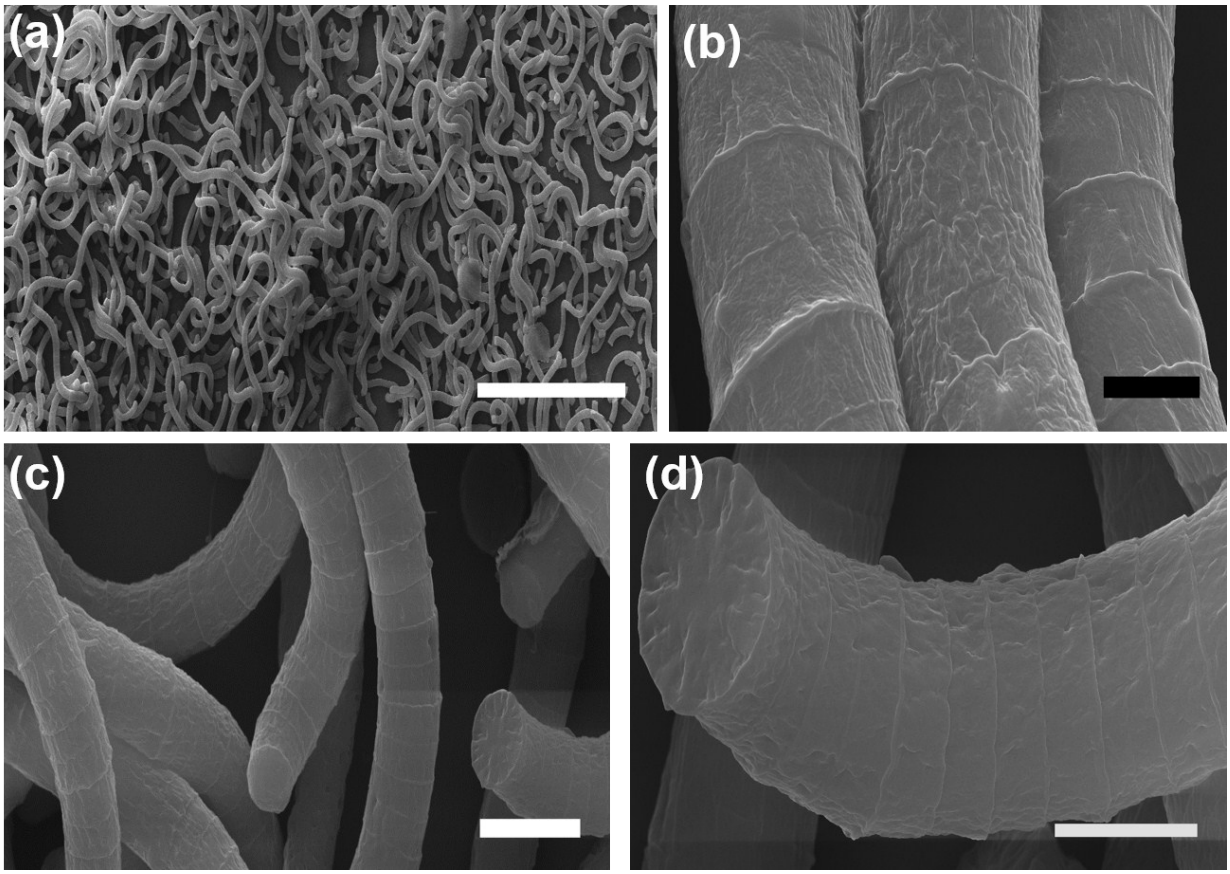

Figure S1: SEM images of helical *Spirulina platensis* bio-template. (a) SEM image showing many overlapping, helical bio-templates. (b-d) SEM images showing a magnified view of the bio-template, clearly depicting the presence of many circular ridges and a rough morphology. Scale bars: (a) 150 µm, (b) 3 µm, (c) 10 µm and (d) 5 µm.

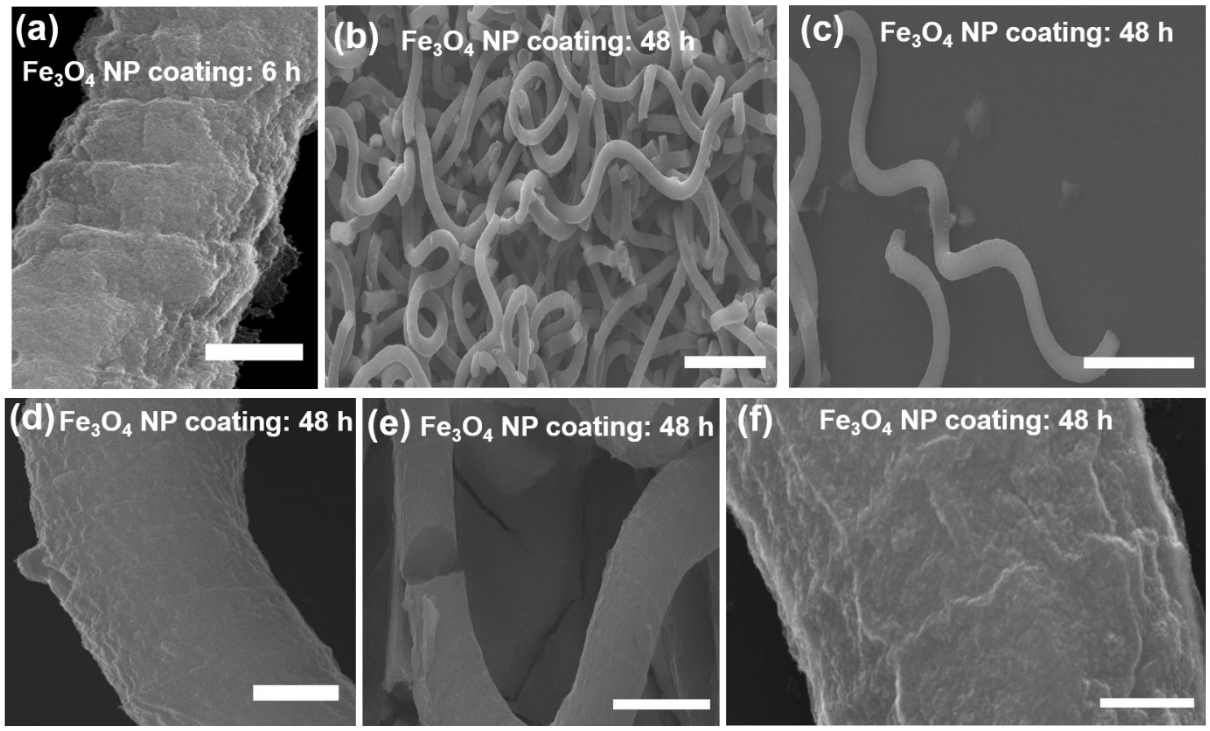

Figure S2: SEM images of Fe_3O_4 NP coated helical bio-templates (a) after 6 hours of coating showing a rough morphology as seen in the bare bio-template. (b-f) SEM images of bio-templates coated for 48 h showing a smooth morphology and even coating of NPs on the helical bio-template. Scale bars: (a) 3 µm, (b)-(c) 40 µm, (d) 4 µm, (e) 10 µm and (f) 1 µm.

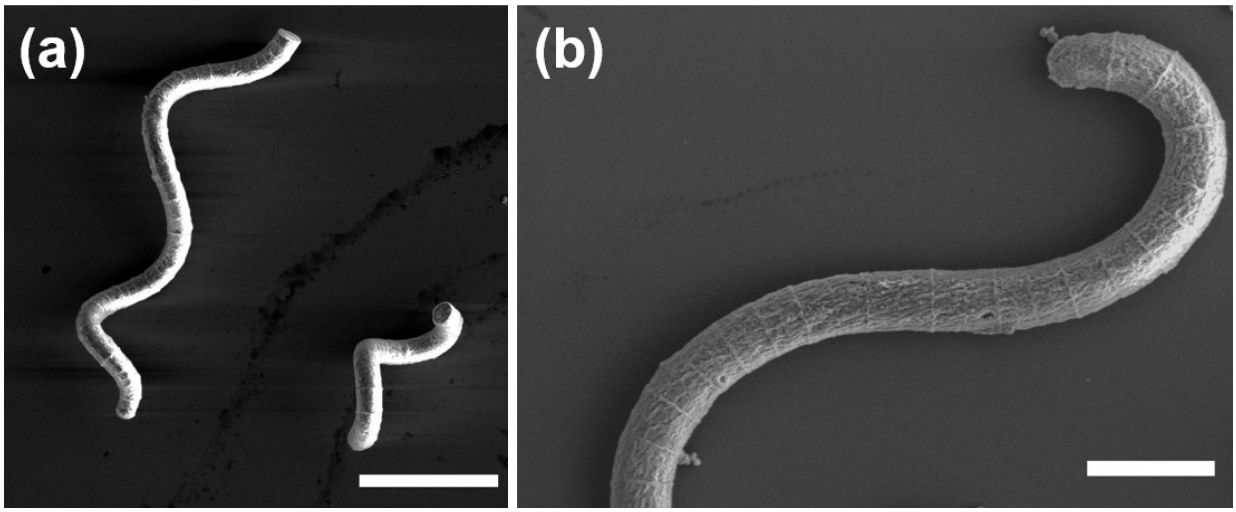

Figure S3: (a,b) SEM images of Fe_3O_4@TiO_x helical bio-templates before annealing showing a uniform coating of the templates with TiO_2. Scale bars: (a) 30 µm and (b) 10 µm.

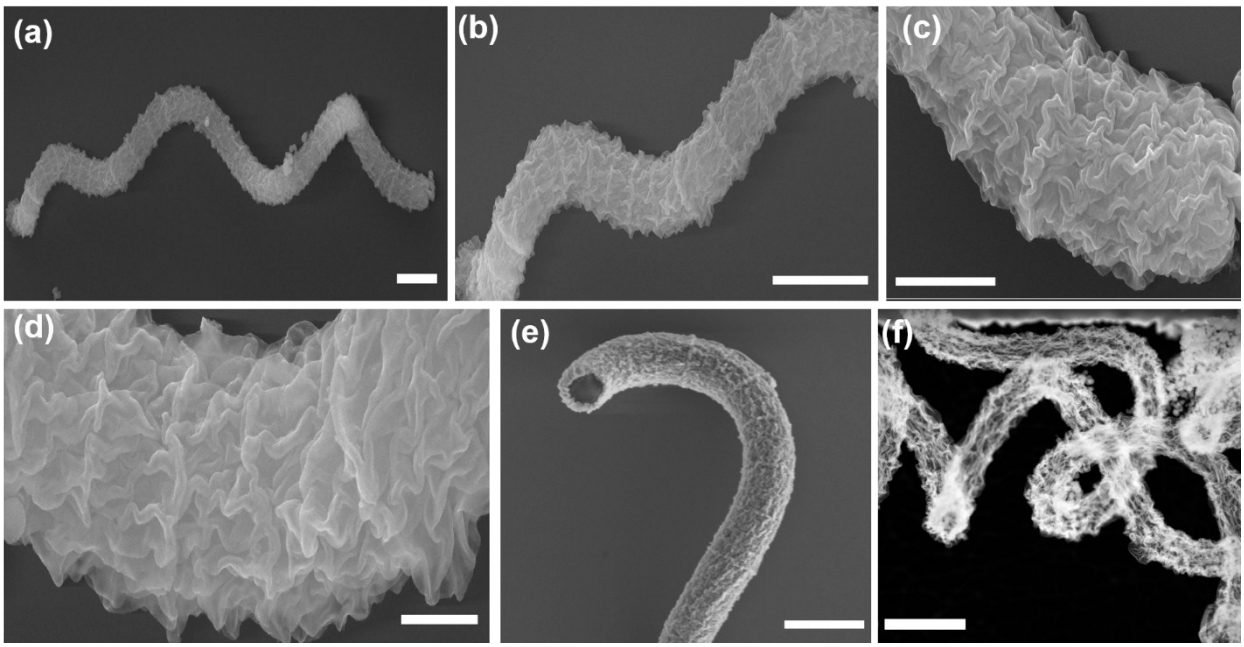

Figure S4: SEM images of annealed hybrid Fe_3O_4@TiO_2 helical bio-templates showing (a, b) that they still retained their helical shape, even after removal of the bio-template. (c, d) SEM images showing a dramatic change in their smooth morphology post-annealing, which is replaced by a very rough surface and (e, f) SEM and TEM images showing development of hollow micro-structures post-annealing. Scale bars: (a) 5 µm, (b) 5 µm, (c) 2 µm, (d) 1 µm, (e) and (f) 5 µm.

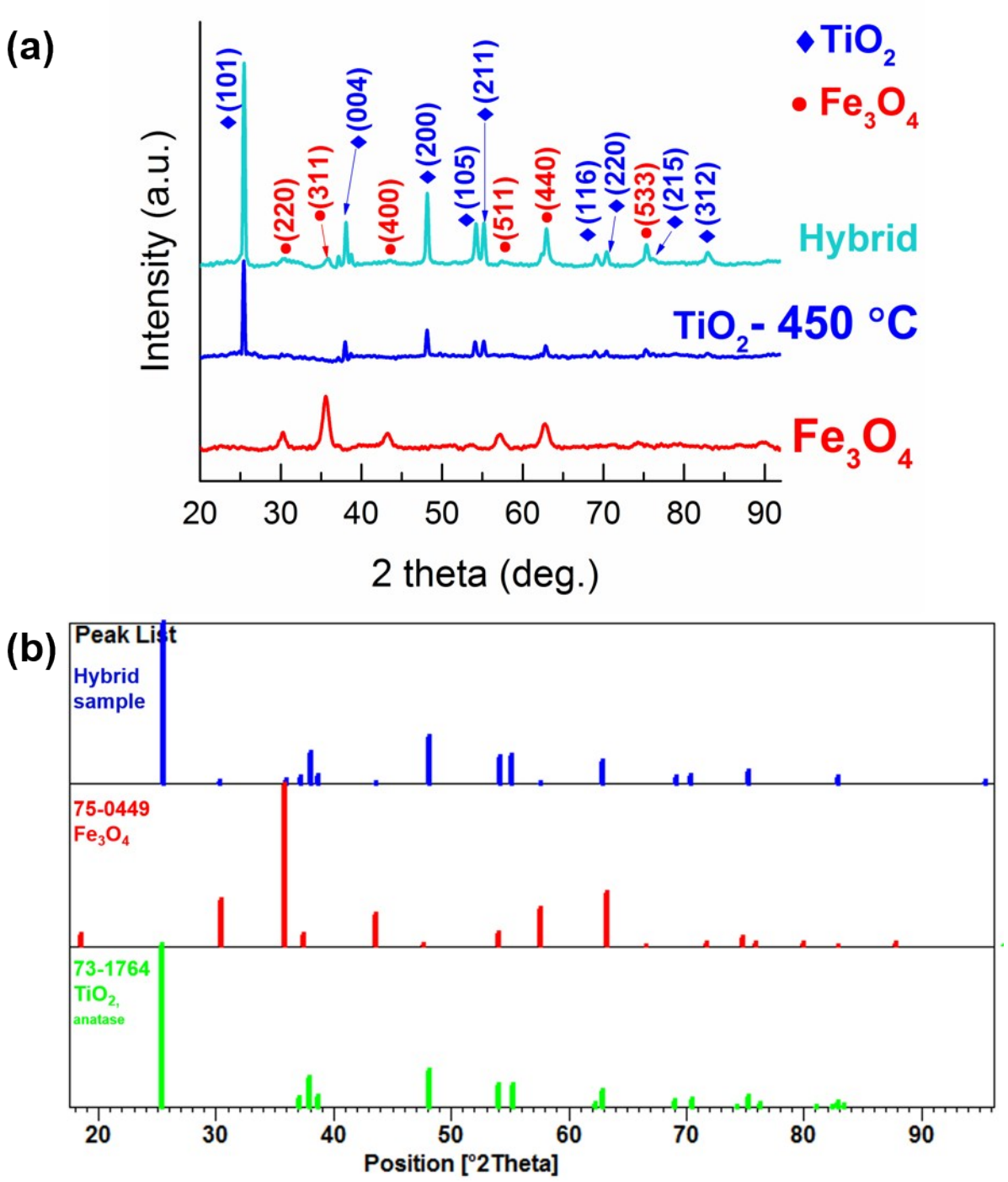

Figure S5: (a) XRD analysis of bio-templates coated with Fe_3O_4 NPs, with TiO_2 and annealed and the hybrid micro-structures after annealing. (b) XRD patterns of hybrid sample and its comparison with the JCPDS patterns of Fe_3O_4 (75-0449) and anatase TiO_2 (73-1764).

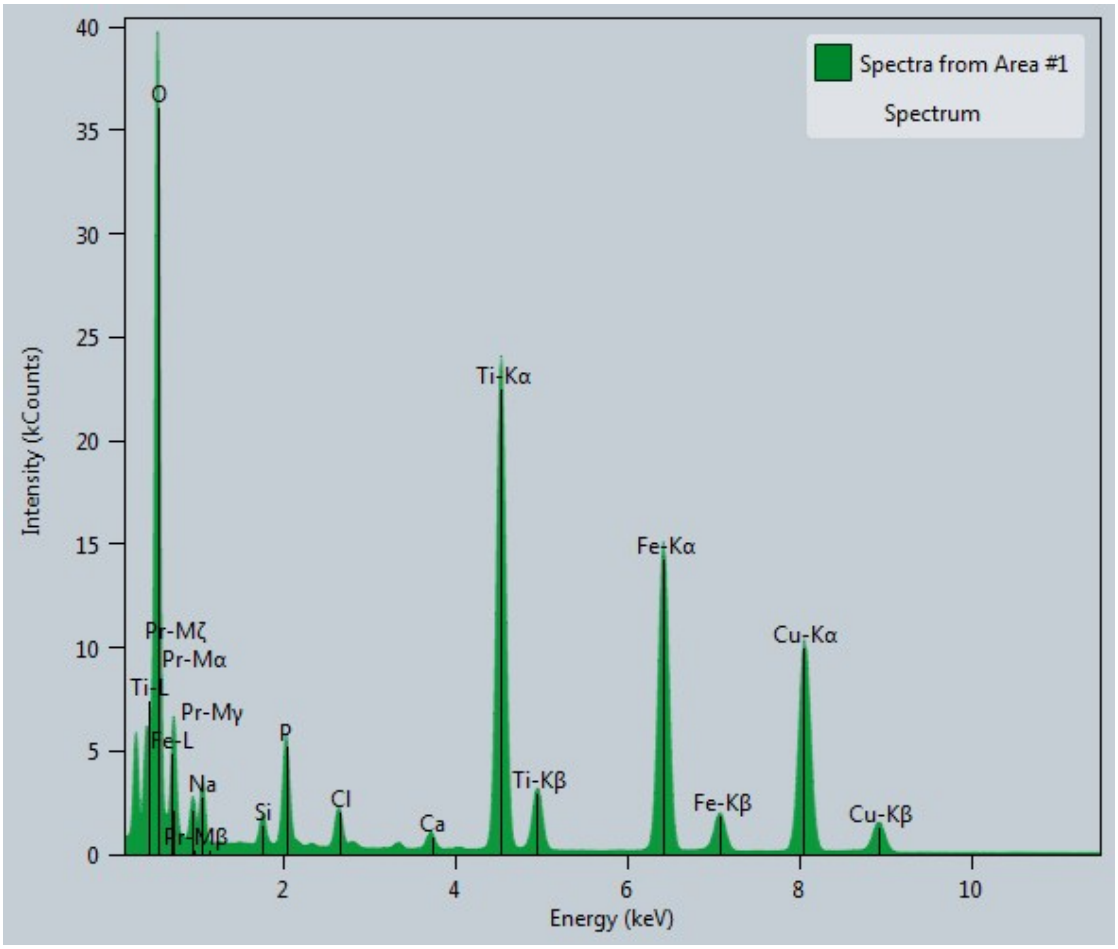

Figure S6: EDX spectrum obtained from hybrid micro-structures after annealing clearly show the presence of peaks arising from Ti, O and Fe.

Architecture/ Composition	**Light source**	**[Pollutant]/ [photocatalyst] (g / g)**	**k-value (min^{-1})**	**Ref**
TiO_2-Fe_3O_4 microhelices	450 W 300 nm < λ < 600	0.01 Rhodamine B	0.047	This work
Ni/PtPd/TiO_2 coaxial nanotubes	450 W, λ > 420 nm,	0.006 Rhodamine B, Methyl Orange Methylene blue	0.0074 (TiO_2 NTs) 0.071 (TiO_2-PtPd NTs)	[1]
BiOCl-Bi_2O_3 micropillars	400 W λ > 400 nm	0.004 Rhodamine B	0.009	[2]
TiO_2-Fe_3O_4 particles	36 W, λ < 400 nm	0.04 Phenol	0.025	[3]
TiO_2-Fe_3O_4 particles	Xenon lamp, 400 W λ > 420 nm	0.02 RhB	0.001 (P25) 0.014 (TiO2-Fe3O4)	[4]
Ag2WO4-Fe_3O_4	300 W Xe lamp, λ > 400 nm	Fast Green	0.0016 (Fe3O4-Ag2WO4)	[5]
Ag3PO4/NiFe2O4	300 W Xe lamp λ > 420 nm	0.04 Methyl Orange	0.03 (Ag3PO4) 0.06 (Ag3PO4-NiFe2O4)	[6]
Fe3O4/ZnO/BiOI/PANI	50 W LED lamp λ > 420 nm	- RhB	0.022 (Fe3O4/ZnO /BiOI/PANI) 0.0003 (Fe3O4/ZnO)	[7]

Table S1. Comparison of organic pollutant degradation performance of other magnetic photocatalysts' with our work.

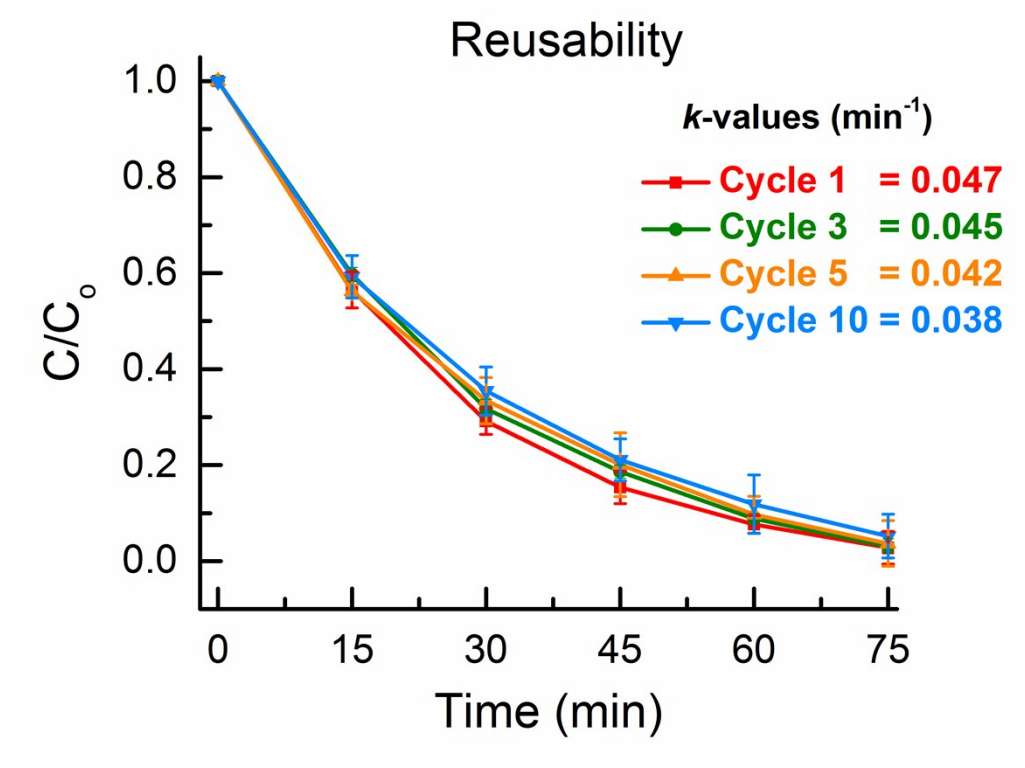

Figure S7: Plot showing results obtained under 10 consecutive cleaning runs using hybrid helices and UV-visible light. From here we can observe that the hybrids displayed a good stability and reusability over multiple runs.

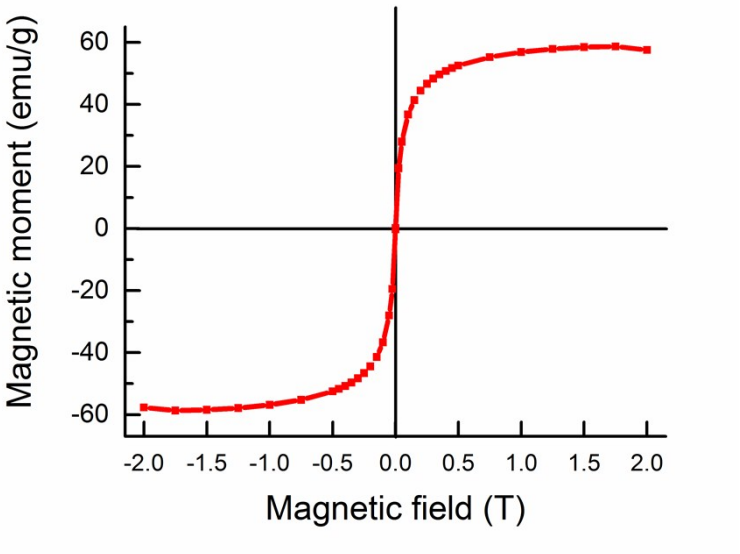

Figure S8: Magnetic hysteresis loop obtained for hybrid microhelices.

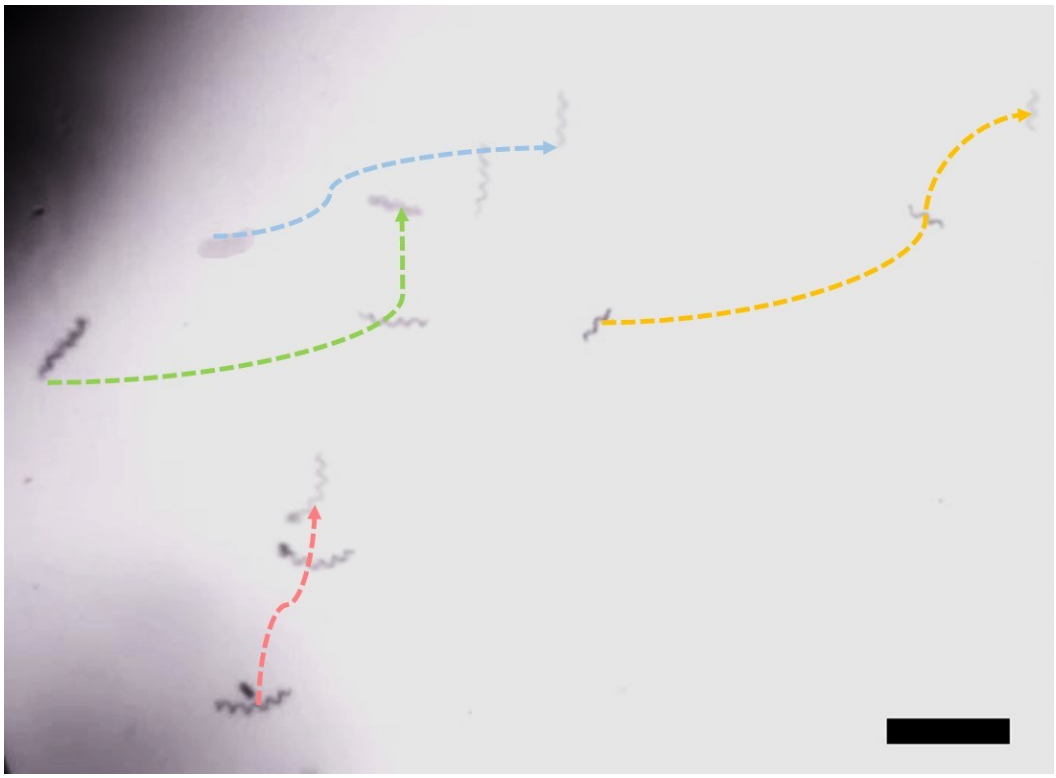

Figure S9: Time-lapse image obtained for a swarm of hybrid microhelices showing their precise propulsion and steering under 10 mT and 12 Hz rotating magnetic fields.

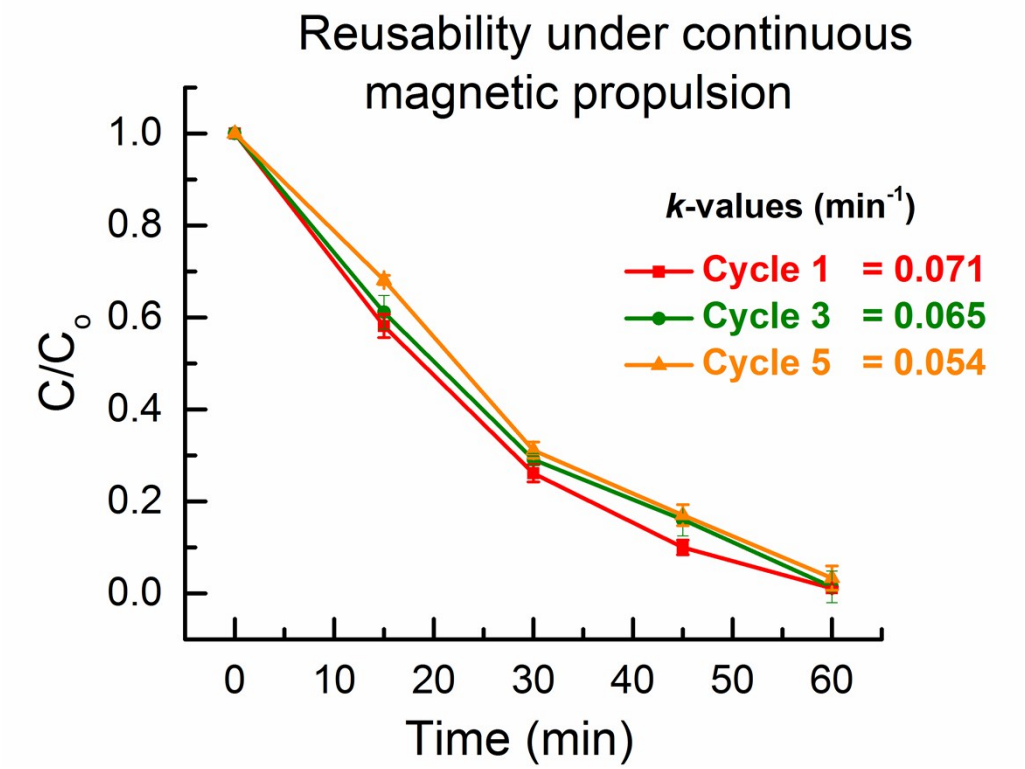

Figure S10. Plot showing results obtained under 5 consecutive cleaning runs using hybrid helices and UV-visible light, under continuous magnetic propulsion.

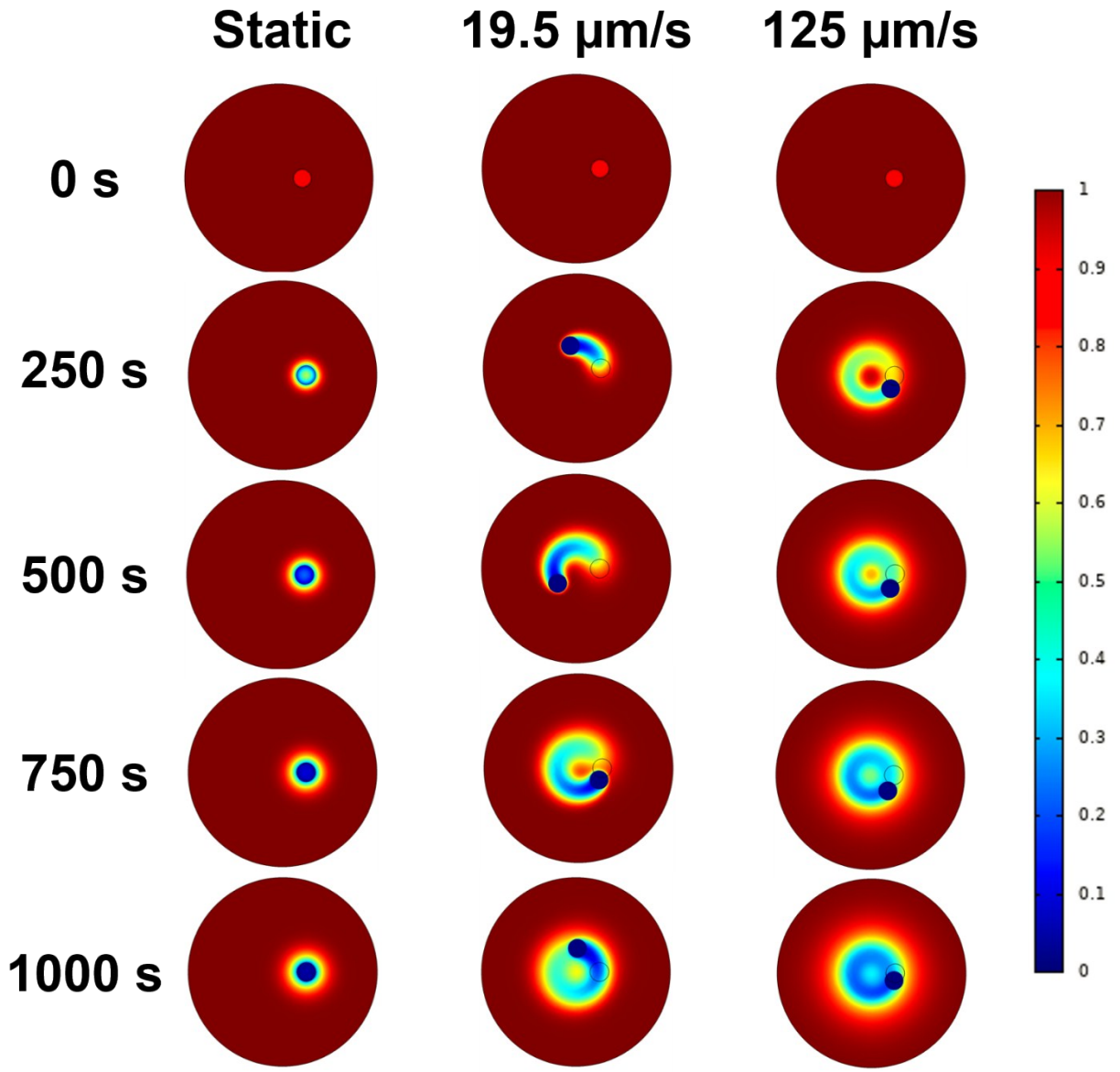

Figure S11: Time-lapse images obtained from COMSOL simulations showing the degradation of organic pollutant obtained under different swimming speeds over 1000 s. The color scale represents the pollutant degradation rates (C/C_o), where maroon color represents $C/C_o=1$ i.e. 100% organic pollutant concentration and dark blue represents complete degradation of organic pollutant.

1. Mushtaq, F.; Asani, A.; Hoop, M.; Chen, X.-Z.; Ahmed, D.; Nelson, B. J.; Pané, S. Highly Efficient Coaxial TiO_2-PtPd Tubular Nanomachines for Photocatalytic Water Purification with Multiple Locomotion Strategies. *Advanced Functional Materials* 2016**,** *26,* 6995-7002.
2. Mushtaq, F.; Guerrero, M.; Sakar, M. S.; Hoop, M.; Lindo, A. M.; Sort, J.; Chen, X.; Nelson, B. J.; Pellicer, E.; Pane, S. Magnetically driven Bi_2O_3/BiOCl-based hybrid microrobots for photocatalytic water remediation. *Journal of Materials Chemistry A* 2015**,** *3,* 23670-23676.
3. Chang, J.; Zhang, Q.; Liu, Y.; Shi, Y.; Qin, Z. Preparation of Fe3O4/TiO2 magnetic photocatalyst for photocatalytic degradation of phenol. *Journal of Materials Science: Materials in Electronics* 2018**,** *29,* 8258-8266.
4. Hong, T.; Mao, J.; Tao, F.; Lan, M. Recyclable Magnetic Titania Nanocomposite from Ilmenite with Enhanced Photocatalytic Activity. *Molecules* 2017**,** *22,* 2044.
5. Rajamohan, S.; Kumaravel, V.; Muthuramalingam, R.; Ayyadurai, S.; Abdel-Wahab, A.; Sub Kwak, B.; Kang, M.; Sreekantan, S. Fe3O4–Ag2WO4: facile synthesis, characterization and visible light assisted photocatalytic activity. *New Journal of Chemistry* 2017**,** *41,* 11722-11730.
6. Huang, S.; Xu, Y.; Zhou, T.; Xie, M.; Ma, Y.; Liu, Q.; Jing, L.; Xu, H.; Li, H. Constructing magnetic catalysts with in-situ solid-liquid interfacial photo-Fenton-like reaction over Ag3PO4@NiFe2O4 composites. *Applied Catalysis B: Environmental* 2018**,** *225,* 40-50.
7. Habibi-Yangjeh, A.; Shekofteh-Gohari, M. Synthesis of magnetically recoverable visible-light-induced photocatalysts by combination of Fe3O4/ZnO with BiOI and polyaniline. *Progress in Natural Science: Materials International* 2019**,** *29,* 145-155.